

Improving Spiking Neural Network Accuracy With Color Model Information Encoded Bit Planes

Nhan T. Luu*, Truong Cong Thang*, Duong T. Luu†

* *Department of Computer Science and Engineering, The University of Aizu, Aizuwakamatsu, Japan*

† *Information and Network Management Center, Can Tho University, Can Tho, Vietnam*

(ltnhan0902@gmail.com, thang@u-aizu.ac.jp, luutd@ctu.edu.vn)

Abstract—Spiking neural networks (SNNs) have emerged as a promising paradigm in computational neuroscience and artificial intelligence, offering advantages such as low energy consumption and small memory footprint. However, their practical adoption is constrained by several challenges, prominently among them being performance optimization. In this study, we present a novel approach to enhance the performance of SNNs through a new encoding method that exploits bit planes derived from various color models of input image data for spike encoding. Our proposed technique is designed to improve the computational accuracy of SNNs compared to conventional methods without increasing model size. Through extensive experimental validation, we demonstrate the effectiveness of our encoding strategy in achieving performance gain across multiple computer vision tasks. To the best of our knowledge, this is the first research endeavor applying color spaces within the context of SNNs. By leveraging the unique characteristics of color spaces, we hope to unlock new potentials in SNNs performance, potentially paving the way for more efficient and effective SNNs models in future researches and applications.

Index Terms—Spiking neural network, spike encoding, image classification

I. INTRODUCTION

The field of artificial intelligence (AI) has experienced unprecedented advancements in recent decades [1], largely driven by the development and optimization of deep learning algorithms. Despite these advancements, traditional artificial neural networks (ANNs) often fall short in modeling the intricate and dynamic nature of biological neural systems [2]. To bridge this gap, spiking neural networks (SNNs) have emerged as a promising alternative, leveraging the temporal dimension of neuronal activity to more closely emulate the behavior of biological brains.

SNNs utilize discrete spike events to transmit information between neurons, mirroring the asynchronous and event-driven communication observed in biological neurons [3]. This approach not only enhances the biological plausibility of neural models but also offers potential advantages in terms of computational efficiency and power consumption, particularly for hardware implementations [4]. The inherent sparsity and temporal coding of SNNs provide a robust framework for developing low-power neuromorphic systems that can operate efficiently in real-time environments [5].

Despite their potential, SNNs pose significant challenges, particularly in training methodologies and network optimization. Traditional backpropagation techniques used in ANNs are not directly applicable to SNNs due to their discontinuous and non-differentiable nature [6]. Consequently, novel training algorithms, such as spike-timing-dependent plasticity (STDP) [7], [8] and surrogate gradient methods [9], have been developed to address these challenges, enabling the effective training of SNNs.

Prior research in ANNs has extensively explored the application of image color spaces to enhance performance across various tasks, demonstrating significant improvements in areas such as image recognition and processing [10], [11]. Motivated by these advancements, we aim to investigate whether these insights on color spaces can similarly improve the performance of SNNs. This led us to formulate our research questions:

- *Does encoding color spaces encapsulate the necessary information to enhance the performance of SNNs?*
- *How can we encode color spaces information into SNNs?*

To answer these hypotheses, we observed that the bit planes of images contain pulse-like information, which has been utilized previously on ANNs [12] and can be apply to encode color spaces information for SNNs to possibly improve accuracy.

II. SPIKING NEURAL NETWORK

In this section we will cover some literature survey related to our research, particularly about SNNs in general and some common knowledge on SNN architecture utilized in our experiments.

A. History of SNNs

Phenomenological neuron models can be progressively simplified until reaching a stage where even neural spikes are not modeled, leading to first and second generation neurons [13], [14]. This simplification significantly reduces computational demands but also decreases biological realism. The detail level in modeling often correlates with available computing power. For example, ANNs based on second generation neurons were historically limited by computing power [15], restricting the size of networks and the complexity of neuronal models. This limitation influenced the design of learning algorithms.

Even with advancements in computing power, the complexity of neuronal models did not proportionately increase because existing learning algorithms were not compatible with more detailed models. Consequently, two distinct research fields emerged.

- *ANNs* [16] focused on large networks of simplified neuron-like units, capable of learning through algorithms like backpropagation, and were successfully applied in pattern recognition, classification, and pattern completion tasks.
- *Computational Neuroscience* [17] in contrast used detailed biophysical and phenomenological models in smaller networks to study electrophysiological processes, pattern generation, and dynamic behaviors of small neuron groups.

Although there have been attempts to create large networks of detailed biophysical neuron models [18], it remains challenging due to computational constraints.

Recent advances in computing power have blurred the lines between these fields. ANNs have become more biologically realistic, while networks of biophysical neurons have grown larger and more detailed. However, computational power still limits the application of detailed models in large neural networks for pattern recognition and classification. With improved computing power, new learning algorithms are being developed for these models. SNNs, which use spiking neurons modeled by phenomenological models like the Spike Response Model [19], represent the next step towards this goal. Due to the computational burden, biophysical models are less common in certain SNN applications. This paper focuses on research involving SNNs with phenomenological models, excluding those using biophysical models.

B. The Integrate-and-Fire model

One of the earliest neuron models is the perfect integrate-and-fire (IF) model (also sometimes referred to as the non-leaky integrate-and-fire model), first studied by Louis Lapicque in 1907 [20]. In this model, the neuron is characterized by its membrane potential V :

$$C \frac{dV(t)}{dt} = I(t) \quad (1)$$

which evolves over time in response to an input current $I(t)$. This evolution is described by the time derivative of the capacitance law, $Q = CV$, where C is the membrane capacitance. As an input current is applied, the membrane potential increases until it reaches a fixed threshold V_{th} . At this point, the neuron generates a spike modeled as a delta function, and the membrane potential is reset to its resting value, after which the process repeats. In this model, the firing rate increases linearly and indefinitely with the increase in input current.

While previous efforts have successfully converted ANN neurons with ReLU activations to IF neurons, challenges still

remain in the conversion process. One of the key issues is the difficulty in precisely determining the appropriate thresholds in these conversion approaches. Despite the introduction of both data-driven and model-driven threshold determination methods [21], the converted SNN often experience unstable accuracy compared to their re-trained ANN counterparts. Additionally, IF neurons lack time-dependent memory. Once a neuron receives sub-threshold potentials, the membrane potential persists without decay until the neuron fires. This behavior is said to be inconsistent with biological neurons, which exhibit dynamic temporal properties [22].

C. Deep Residual Learning in Spiking Neural Networks

The success of ResNet [23] in deep learning has motivated efforts to extend residual learning to SNN. Prior attempts, commonly referred to as Spiking ResNets [24], have largely replicated the architecture of ResNet [23] by replacing ReLU activation functions with spiking neurons. However, this approach presents certain limitations:

- *Inability to achieve identity mapping across neuron models*: Residual learning is predicated on the concept of identity mapping, where layers can be trained to approximate an identity function. While this is straightforward in ResNets [23] with ReLU activation, it is not always feasible in Spiking ResNets [24]. Specifically, [25] claimed that for certain spiking neuron models, such as leaky integrate-and-fire (LIF) neurons [20] with learnable membrane time constants, ensuring that a spiking neuron fires in response to an input spike becomes challenging. This complicates the realization of identity mapping.
- *Vanishing/exploding gradients*: Even in cases where identity mapping can be achieved, Spiking ResNets [24] are prone to vanishing or exploding gradients during training. This occurs because the gradient propagation through multiple layers of spiking neurons may either diminish to zero or grow uncontrollably, complicating the training of deeper networks.

To address these issues, SEW ResNet [25] was introduced as a replacement design for residual blocks while utilizing IF neurons. The SEW block capitalizes on the binary nature of spikes by applying element-wise functions g to the output of the residual mapping $A_l[t]$ and the input spike train $S_l[t]$ [25]. This approach facilitates identity mapping, mitigates the vanishing/exploding gradient problem and achieves higher accuracy with fewer time steps compared to existing SNN models. With these advantages in mind, we have decided to choose (but not limited to) SEW Resnet [25] architecture as our main experimenting architecture.

III. SPIKE CODING IN SNNs

In the context of SNN there are several encoding methods, each with unique advantages and disadvantages.

- *Rate coding* [26], [27] is the predominant coding technique utilized for spikes in SNNs. In rate coding, the

number of spikes within a specific time interval is counted, and the firing rate is interpreted as the signal intensity. This method inherently includes a high level of redundancy and exhibits tolerance to a certain degree of noise.

- *Temporal coding* [3] is the form of coding where spike patterns are distributed over time. Population-based coding methods [28] encode information based on the number of spikes within a given time frame. In contrast, interspike interval methods [29] use the time between two spikes as their coding scheme. Temporal coding allows for arbitrarily sized data patterns, though longer patterns require extended time periods.

We primarily focus on *rate coding*, as it is one of the most widely used encoding schemes in conventional SNNs for representing signals with spike trains. In the *rate coding* scheme, the firing frequency of a neuron represents the signal intensity. The firing rate r_i of the i -th neuron provided by [30] can be expressed as follows:

$$r_i = \frac{N_s}{T} = \frac{\sum_{t=1}^T s_i(t)}{T} \quad (2)$$

When N_s spikes are fired over T time steps, each time step can either produce a spike or none. The firing rate is 1 if a neuron fires at every time step, and 0 if it does not fire at all. In image classification, for instance, if a pixel intensity ranges [0.0, 1.0], it can be represented by a spike train with a corresponding firing rate [0.0, 1.0] as input to the SNN.

In this research, we will be using the *Poisson-distributed rate coding* [30], [31] scheme where spike s_i for i -th pixel with intensity P_i can be interpreted as:

$$s_i = \begin{cases} 1 & \text{if } \text{random}(0.0, 1.0) \geq P_i \\ 0 & \text{otherwise} \end{cases} \quad (3)$$

IV. COLOR SPACES AND THEIR APPLICATION IN DEEP LEARNING

This section will provide an overview of relevant concepts for our research, focusing specifically on the color models explored and their applications in deep learning algorithms.

A. Color spaces

Color spaces are fundamental in computer graphics as they define how colors are represented, manipulated, and displayed within digital images. In computer graphics applications, understanding and effectively managing color spaces is crucial for tasks such as rendering realistic scenes, creating digital artwork, and designing user interfaces. In this subsection, we will discuss the color spaces under investigation in our experiments, divided by certain criteria from [32], [33], including: *device-oriented models*, *user-oriented models* and *device-independent models*.

1) *Device-oriented models*: These models are influenced by the signals of the devices and the resulting colors are affected by the tools used for display. Widely utilized in various applications that require color consistency with hardware tools, examples include any hardware devices used for human visual perception, such as televisions and video systems. While there are different models for separate use-cases and devices, for now we will only concern with RGB, CMY(K) and YCbCr.

2) *User-oriented models*: User-oriented color models are considered as a pathway between the observer and the device handling the color information. These models enable users to describe and approximate their color perceptions from the presented colors. For our experiments, we mostly investigate cylindrically described models, including HSL and HSV. According to [32], these models also inherit other special properties such as devices dependence and cylindrical-coordinate representation.

3) *Device-independent models*: Device-independent color models are essential for defining color signals without reliance on the specific characteristics of any particular device or application. These models play a crucial role in applications that involve color comparisons and the transmission of visual information across networks that connect various hardware platforms. We will mostly research color spaces defined by the International Commission on Illumination (CIE), including CIE XYZ and CIE LAB.

B. Usage of color models in deep learning

Color models are becoming increasingly important in deep learning algorithms, offering valuable information that enhances model performance in various tasks. For example, research on traffic light recognition [34] tested a range of color models across different deep learning architectures, with results indicating that the RGB model remains favored despite some of its limitations. This suggests that, while RGB is not perfect, it still outperforms other models in certain applications.

In another study focused on applying convolutional neural networks (CNNs) for skin detection against adversarial attacks of generative models [35], RGB and YCbCr color models demonstrated superior performance, particularly in handling varying lighting conditions. This highlights the adaptability of these color models in scenarios where lighting inconsistencies can degrade model accuracy.

Moreover, the development of ColorNet [10] illustrates the potential of leveraging multiple color spaces to capture a broader set of features. By combining information from these diverse color spaces, ColorNet outperforms traditional models that rely on a single color space. However, this approach introduces computational overhead due to the inclusion of smaller submodels, which can be a challenge despite the model's increased efficiency in some cases.

Despite extensive researches on the use of color models in ANNs, their application in SNNs remains underexplored and requires further investigation.

V. BIT PLANES APPLICATION IN DEEP LEARNING

Bit planes have shown extensive utility in deep learning applications, offering new ways to improve model efficiency and performance. In one study, researchers used bit planes to encode the input layer in Binary Neural Networks (BNNs) [12]. They argued that bit planes retain crucial spatial information, enabling a reduction in the number of multiply-accumulate operations (MACs) without compromising the model’s accuracy or robustness. This demonstrates the potential of bit planes in streamlining computations while maintaining competitive performance.

Another study explored the use of bit plane slicing on RGB images for adversarial robustness [36]. By selecting the most significant bit planes, the researchers developed a classification model that was better equipped to handle adversarial attacks. This approach capitalizes on the spatial information encoded in different bit planes, which helps the model resist manipulations that would otherwise degrade its performance.

In the domain of medical imaging, bit plane slicing has also been applied to improve accuracy in breast cancer recognition tasks [37]. Researchers found that lower-order bit planes are more susceptible to noise, and by removing them before inputting the data into a convolutional neural network (CNN), they achieved higher classification accuracy. This method highlights how bit plane analysis can be tailored to specific challenges, such as noise reduction in medical images, to enhance model effectiveness.

Similar to color models, although bit planes have been widely studied and applied in ANNs, their utilization in SNNs is still relatively unexplored and demands further research.

VI. EXPERIMENTS SETUP

In this section, we will discuss in details about the implementation of our encoding algorithm and setup for experimenting with this method.

A. Preliminary testing

As theoretically mentioned in [38] and practically measured in [39], [40], a Poisson-distributed time steps appear to positively correlate with training accuracy in SNNs and to achieve a correct spike distribution, the input must be sampled to a certain frequency. However in the case of a high time steps input, this approach sacrifices the energy efficiency of SNNs, which is one of their primary advantages. Despite this trade-off, the improvement in training accuracy suggests that the benefits in performance might outweigh the costs in specific applications where accuracy is paramount.

We previously hypothesize that the information contained in the bit planes of color models can be effectively used to encode inputs for SNN training. Bit planes decompose an image into

binary levels, each representing a specific bit of the pixel values. This decomposition can potentially preserve critical information from the original image while providing a format that might be more suitable for the spike-based processing in SNNs. The granularity of information available in bit planes offers a unique approach to encoding visual data, which could enhance the learning capabilities of SNNs by providing a richer, multi-level representation of the input.

To test our hypotheses, we conducted preliminary experiments using the CIFAR-10 dataset, employing the bit plane encoding method. We compared this approach with traditional rate coding and a combination of both methods (illustrated in details in Figure 2 and Section VI-B) with a rate coding step size $T = 10$ (illustrated in Figure 1 and Table I).

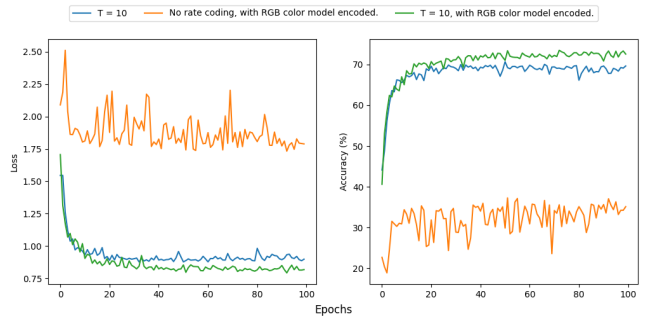


Fig. 1: Compare training progression on CIFAR-10 [41] between using traditional rate coding (denoted blue), encoding using only bit planes information (denoted orange) and combining bit planes information with rate coding (denoted green).

| Encoding method | Validation Accuracy (%) |
|-------------------------------------------------------------------------------|-------------------------|
| Poisson rate coding with time step $T=10$ | 70.69 |
| RGB bit plane encoding | 73.49 |
| Poisson rate coding with time step $T=10$ and combined RGB bit plane encoding | 37.28 |

TABLE I: Validation accuracy comparison on CIFAR-10 [41] between traditional rate coding, encoding using only bit planes information and combining bit planes information with rate coding.

Visible from our results, feeding bit plane information of the encoded RGB color model to the SNNs allowed the model to converge to a certain level of accuracy. Still, the accuracy of purely bit planes encoded inputs still fall short compare to rate coding. On the other hand, a combination of rate coding and bit planes encoding experience an increase in performance, this outcome demonstrates that bit planes in color models contain valuable information that SNNs can learn from to improve their classification ability and encourage us to perform testing on other datasets with different color models (as mentioned in Section IV-A).

B. Overall encoding scheme with color spaces

As we can see in Figure 2, for our research the encoding scheme adopted integrates a dual approach featuring both traditional rate coding and bit plane encoding methodologies. Initially, the process commences with the conventional rate coding procedure applied to the image tensor. Subsequently, depending on the chosen color model (for example RGB), the image tensor may undergo conversion to the specified model or proceed directly to encoding if already in RGB format. Following this, the bit plane encoding algorithm (will be discussed in details in Section VI-C and Algorithm 1) is employed to transform the color-modeled image into binary planes. The final encoded tensors are then generated through tensor concatenation across the first dimension, merging the outputs from rate coding and bit plane encoding. These encoded tensors are thereby prepared for utilization in inference tasks and/or training processes, facilitating enhanced performance in our computational models.

C. Bit plane encoding algorithm

To achieve our research objectives, we have developed Algorithm 1 designed to encode an image tensor batch X into n_{bit} bit planes. To determine n_{bit} , it is essential to know the maximum possible value X_{max} of the tensor batch. Since different color models have varying X_{max} , this value must be predefined according to the selected color model (for example, if RGB is chosen, then $X_{max} = 255$). Once X_{max} is defined, n_{bit} can be calculate as $\lceil \log_2(X_{max}) \rceil$.

To calculate the bit planes of an unnormalized integer input tensor batch X , we perform element-wise division of X by 2. The remainder from this division constitutes a bit plane of X , while the quotient is saved for the extraction of subsequent bit planes. This process is repeated until we obtain n_{bit} bit planes. The resulting bit planes are then concatenated to form a binary tensor batch with the shape (n_{bit}, B, C, H, W) . This format closely resembles that of rate encoding and ensures determinism in the encoding results without having to sample more than n_{bit} times.

D. Experiment setup

To investigate performance gains during training process, the experimented model should be a medium-sized SNN with potential for improvement in computer vision tasks. After careful consideration, we had decided to select SEW-ResNet18 with ADD element-wise function [25] which is a novel medium size SNN tested on various computer vision tasks and suitable to our specifications. The model and experiment process was implemented using PyTorch [42] and SpikingJelly [43], incorporating color conversion algorithms based on implementations from Kornia [44]. During the rate coding steps, all training processes utilized step size $T = 10$. For optimization, we employed the Adam optimizer [45] with a learning rate of $lr = 1e - 3$ and $\beta = (0.9, 0.999)$ for all tested datasets. Cross-Entropy Loss with Softmax function and

Algorithm 1 Bit plane encoding algorithm

Require: $X_{shape} \in (B, C, H, W)$ \triangleright Constraining input format of multiple images. If input is a single image we should have $B = 1$.
Require: X_{max} is defined
function BIPLANEENCODE(X, X_{max})
 $n_{bit} \leftarrow \lceil \log_2(X_{max}) \rceil$ \triangleright Get number of bit required to encode image from highest possible value X .
 $L \leftarrow []$ \triangleright Empty list initialization.
for $i \leftarrow 0, i < n_{bit}, i + +$ **do**
 $L.insert(X \bmod 2)$ \triangleright Element-wise modulo of tensor, then store the bit plane.
 $X \leftarrow \lfloor X/2 \rfloor$ \triangleright Element-wise division of tensor.
end for
return $concat(L)$ \triangleright Return a concatenated tensor batches of new dimension (n_{bit}, B, C, H, W)
end function

mean reduction $L(x, y)$ [42] across N mini-batch dimension was also widely employed as the loss function:

$$L(x, y) = \frac{\sum_{n=1}^N l_n}{N}, \quad (4)$$

$$l_n = - \sum_{c=1}^C w_c \log \frac{\exp\{x_{n,c}\}}{\sum_{i=1}^C \exp\{x_{n,i}\}} y_{n,c}$$

with l_n is loss of each mini-batch, x is the input, y is the target, w is the weight, total amount of class C where mini-class $c, i \in C$.

VII. RESULTS

In this section we will discuss results of our main experiments along with some interesting findings beside original hypotheses.

A. The effect of bit plane encoding on colored images

For our experiment, we conducted tests on various image classification datasets, including CIFAR10 [41], CIFAR100 [41], EuroSAT [46], Caltech101 [47], Caltech256 [48], Imagenette [49] (which is a subset of ImageNet [50]), GTSRB [51], and Food101 [52]. We allocated 80% of each dataset for training and the remaining 20% for validation. All datasets were processed with a batch size of 16 images for 100 epochs on an NVIDIA RTX 3090 GPU, where CIFAR10 [41], CIFAR100 [41] and EuroSAT [46] are trained on original input size while input of all other dataset are resize to 224x224 pixels.

As depicted in Table II, the average accuracy and loss curves across all tested color models demonstrated improved performance. Despite a deterministic increase in inference time and input size, the results indicate that the information extracted from color model bit planes enhanced the training

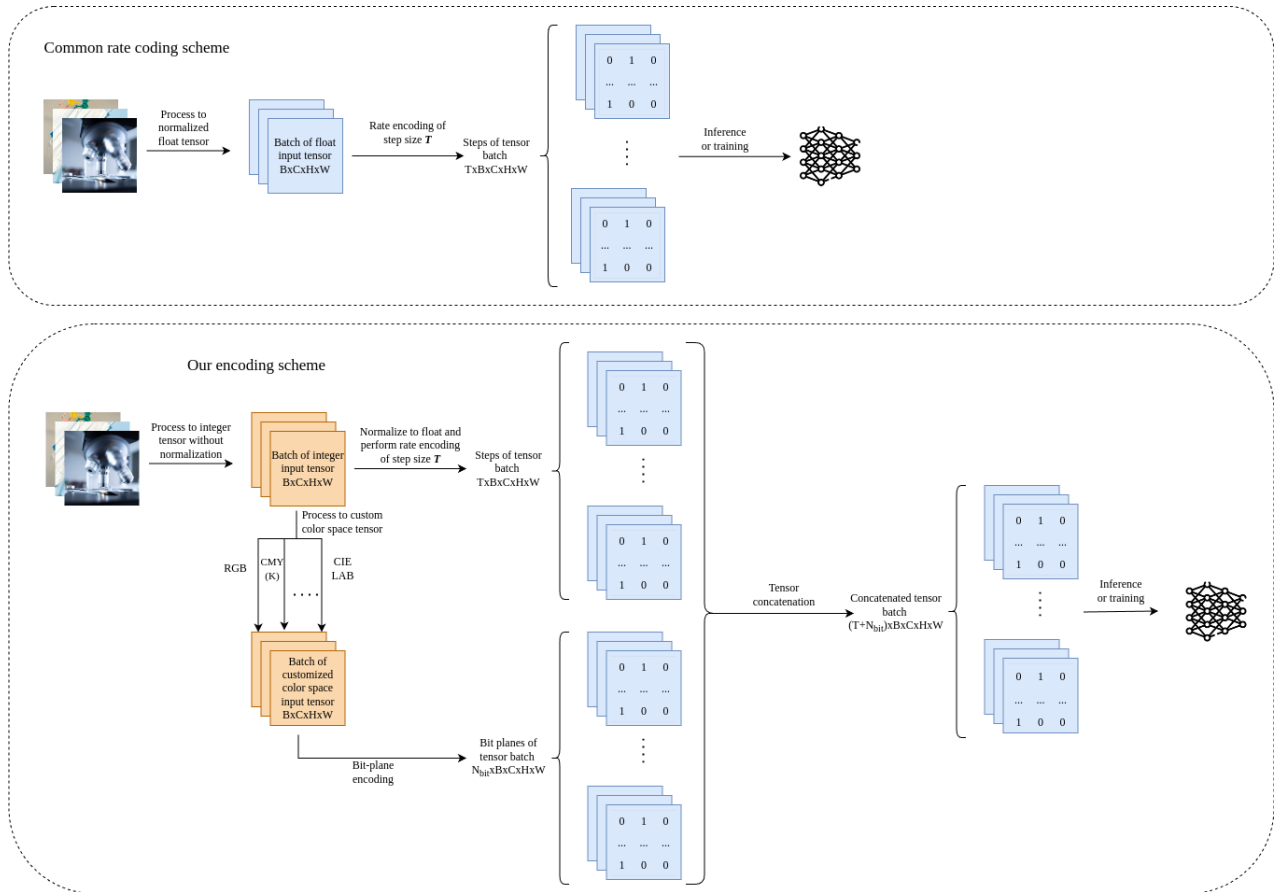


Fig. 2: Our proposed encoding method (lower) compare with traditional rate coding method (upper).

process. This enhancement serves as an information supplement, leading to higher performance overall without increasing the model size.

B. The effect of bit plane encoding on low resolution grayscale images

| Dataset | Accuracy of encoding methods (%) | | |
|--------------------|-----------------------------------------|-----------------------------------------------------------------------------|--------------------------------------------|
| | Poisson rate coding with time step T=10 | Poisson rate coding with time step T=10 and combined RGB bit plane encoding | RGB bit plane encoding with no rate coding |
| MNIST [53] | 98.43 | 98.51 | 97.63 |
| Fashion-MNIST [54] | 87.99 | 88.78 | 85.76 |
| KMNIST [55] | 93.85 | 94.60 | 91.39 |

TABLE III: Comparison of best validation accuracy in percentage between encoding methods, best performing model is emphasized.

Our encoding scheme is designed to leverage color information to enhance the performance of SNN models,

which is why testing on grayscale images was not initially prioritized. However, given that bit-plane encoding can be feasibly applied to single-channel grayscale images, we aim to investigate whether this approach yields any significant or insightful results. Although grayscale images consist of a pixel intensity range between $[0, 255]$, we can adapt our encoding process by applying RGB-based encoding with a reduced number of channels. This method would produce eight bit-plane channels that represent the image information in binary form.

As demonstrated in Table III (for further details see Figure 5 in Appendix A), the combination of Poisson rate coding with bit-plane encoding outperformed other coding methods in terms of validation accuracy. Notably, using only bit-plane information resulted in only a slight reduction in accuracy. As discussed in the previous section, we hypothesize that although bit-plane encoding contains less information compared to traditional rate coding, the model can still converge to a certain extent in computer vision tasks. We further suspect that this performance deficit may be less pronounced in less complex tasks (in this situation, is a low resolution grayscale image recognition task).

| Dataset | Accuracy of encoding methods (%) | | | | | | | |
|-----------------|----------------------------------|-------------------------|-------------------------|---------------------------|-------------------------|-------------------------|-----------------------------|-----------------------------|
| | Poisson rate coding | With RGB encoded (Ours) | With CMY encoded (Ours) | With YCbCr encoded (Ours) | With HSL encoded (Ours) | With HSV encoded (Ours) | With CIE XYZ encoded (Ours) | With CIE LAB encoded (Ours) |
| CIFAR10 [41] | 70.69 | 73.49 | 73.06 | 73.64 | 73.39 | 73.06 | 73.63 | 74.06 |
| CIFAR100 [41] | 38.57 | 42.15 | 41.31 | 41.62 | 41.94 | 41.91 | 41.73 | 42.03 |
| Caltech101 [47] | 61.67 | 64.55 | 65.65 | 65.53 | 66.46 | 68.41 | 65.30 | 66.22 |
| Caltech256 [48] | 30.04 | 41.51 | 40.65 | 40.84 | 40.55 | 39.94 | 40.50 | 40.79 |
| EuroSAT [46] | 84.39 | 88.48 | 86.61 | 88.11 | 88.74 | 88.81 | 88.87 | 87.48 |
| Imagenette [49] | 72.99 | 78.68 | 77.35 | 78.78 | 78.55 | 78.50 | 77.35 | 78.70 |
| Food101 [52] | 19.62 | 36.95 | 37.71 | 36.98 | 38.03 | 36.41 | 37.10 | 35.87 |
| GTSRB [51] | 93.36 | 95.35 | 51.36 | 70.68 | 79.18 | 80.86 | 51.78 | 51.78 |

TABLE II: Comparison of best validation accuracy in percentage between traditional rate coding method and our encoding methods, best performing model is emphasized.

VIII. CONCLUSION

In conclusion, our research introduces a novel encoding method for SNN that leverages bit planes derived from various color models of input image data. This approach prove to enhances the computational accuracy of SNN without increasing the model size. Through extensive experimental validation, we have demonstrated the effectiveness of our encoding strategy across multiple computer vision tasks, achieving notable performance gains compared to conventional methods. This study is pioneering in its application of color spaces within the context of spiking neural networks, and we believe that our findings open new avenues for the development of more efficient and effective SNN models. Our work sets a foundation for future research and applications, potentially advancing the field of computational neuroscience and artificial intelligence.

REFERENCES

- [1] M. A. Wani, F. A. Bhat, S. F. Afzal, and A. I. Khan, *Advances in deep learning*. Springer, 2020.
- [2] D.-A. Nguyen, X.-T. Tran, and F. Iacopi, "A review of algorithms and hardware implementations for spiking neural networks," *Journal of Low Power Electronics and Applications*, vol. 11, no. 2, p. 23, 2021.
- [3] D. Auge, J. Hille, E. Mueller, and A. Knoll, "A survey of encoding techniques for signal processing in spiking neural networks," *Neural Processing Letters*, vol. 53, no. 6, pp. 4693–4710, 2021.
- [4] P. Blouw, X. Choo, E. Hunsberger, and C. Eliasmith, "Benchmarking keyword spotting efficiency on neuromorphic hardware," in *Proceedings of the 7th annual neuro-inspired computational elements workshop*, 2019, pp. 1–8.
- [5] B. Rajendran, A. Sebastian, M. Schmuker, N. Srinivasa, and E. Eleftheriou, "Low-power neuromorphic hardware for signal processing applications: A review of architectural and system-level design approaches," *IEEE Signal Processing Magazine*, vol. 36, no. 6, pp. 97–110, 2019.
- [6] J. D. Nunes, M. Carvalho, D. Carneiro, and J. S. Cardoso, "Spiking neural networks: A survey," *IEEE Access*, vol. 10, pp. 60 738–60 764, 2022.
- [7] G. Srinivasan, S. Roy, V. Raghunathan, and K. Roy, "Spike timing dependent plasticity based enhanced self-learning for efficient pattern recognition in spiking neural networks," in *2017 International Joint Conference on Neural Networks (IJCNN)*. IEEE, 2017, pp. 1847–1854.
- [8] F. Liu, W. Zhao, Y. Chen, Z. Wang, T. Yang, and L. Jiang, "Sstdp: Supervised spike timing dependent plasticity for efficient spiking neural network training," *Frontiers in Neuroscience*, vol. 15, p. 756876, 2021.
- [9] E. O. Neftci, H. Mostafa, and F. Zenke, "Surrogate gradient learning in spiking neural networks: Bringing the power of gradient-based optimization to spiking neural networks," *IEEE Signal Processing Magazine*, vol. 36, no. 6, pp. 51–63, 2019.
- [10] S. N. Gowda and C. Yuan, "Colormet: Investigating the importance of color spaces for image classification," in *Computer Vision–ACCV 2018: 14th Asian Conference on Computer Vision, Perth, Australia, December 2–6, 2018, Revised Selected Papers, Part IV 14*. Springer, 2019, pp. 581–596.
- [11] J. Taipalmaa, N. Passalis, and J. Raitoharju, "Different color spaces in deep learning-based water segmentation for autonomous marine operations," in *2020 IEEE international conference on image processing (ICIP)*. IEEE, 2020, pp. 3169–3173.
- [12] L. Vorabbi, D. Maltoni, and S. Santi, "Input layer binarization with bit-plane encoding," in *International Conference on Artificial Neural Networks*. Springer, 2023, pp. 395–406.
- [13] S. Ghosh-Dastidar and H. Adeli, "Spiking neural networks," *International journal of neural systems*, vol. 19, no. 04, pp. 295–308, 2009.
- [14] W. Maass, "Networks of spiking neurons: the third generation of neural network models," *Neural networks*, vol. 10, no. 9, pp. 1659–1671, 1997.
- [15] N. C. Thompson, K. Greenewald, K. Lee, and G. F. Manso, "The computational limits of deep learning," *arXiv preprint arXiv:2007.05558*, vol. 10, 2020.
- [16] I. Goodfellow, Y. Bengio, and A. Courville, *Deep learning*. MIT press, 2016.
- [17] T. J. Sejnowski, C. Koch, and P. S. Churchland, "Computational neuroscience," *Science*, vol. 241, no. 4871, pp. 1299–1306, 1988.
- [18] A. Zjajo, J. Hofmann, G. J. Christiaanse, M. Van Eijk, G. Smaragdos, C. Strydis, A. De Graaf, C. Galuzzi, and R. Van Leuken, "A real-time reconfigurable multichip architecture for large-scale biophysically accurate neuron simulation," *IEEE transactions on biomedical circuits and systems*, vol. 12, no. 2, pp. 326–337, 2018.
- [19] W. Gerstner, "Spike-response model," *Scholarpedia*, vol. 3, no. 12, p. 1343, 2008.
- [20] L. F. Abbott, "Lapicque's introduction of the integrate-and-fire model neuron (1907)," *Brain research bulletin*, vol. 50, no. 5-6, pp. 303–304, 1999.
- [21] P. U. Diehl, D. Neil, J. Binas, M. Cook, S.-C. Liu, and M. Pfeiffer, "Fast-classifying, high-accuracy spiking deep networks through weight and threshold balancing," in *2015 International joint conference on neural networks (IJCNN)*. IEEE, 2015, pp. 1–8.
- [22] L. Zhang, S. Zhou, T. Zhi, Z. Du, and Y. Chen, "Tdsnn: From deep neural networks to deep spike neural networks with temporal-coding," in *Proceedings of the AAAI conference on artificial intelligence*, vol. 33, no. 01, 2019, pp. 1319–1326.
- [23] K. He, X. Zhang, S. Ren, and J. Sun, "Deep residual learning for image recognition," in *Proceedings of the IEEE conference on computer vision and pattern recognition*, 2016, pp. 770–778.
- [24] Y. Hu, H. Tang, and G. Pan, "Spiking deep residual networks," *IEEE Transactions on Neural Networks and Learning Systems*, vol. 34, no. 8, pp. 5200–5205, 2021.
- [25] W. Fang, Z. Yu, Y. Chen, T. Huang, T. Masquelier, and Y. Tian, "Deep residual learning in spiking neural networks," *Advances in Neural Information Processing Systems*, vol. 34, pp. 21 056–21 069, 2021.
- [26] W. Gerstner and W. M. Kistler, *Spiking neuron models: Single neurons, populations, plasticity*. Cambridge university press, 2002.

- [27] W. Gerstner, W. M. Kistler, R. Naud, and L. Paninski, *Neuronal dynamics: From single neurons to networks and models of cognition*. Cambridge University Press, 2014.
- [28] W. J. Ma, "Signal detection theory, uncertainty, and poisson-like population codes," *Vision research*, vol. 50, no. 22, pp. 2308–2319, 2010.
- [29] F. Ponulak and A. Kasinski, "Introduction to spiking neural networks: Information processing, learning and applications," *Acta neurobiologicae experimentalis*, vol. 71, no. 4, pp. 409–433, 2011.
- [30] J. Kim, H. Kim, S. Huh, J. Lee, and K. Choi, "Deep neural networks with weighted spikes," *Neurocomputing*, vol. 311, pp. 373–386, 2018.
- [31] D. Heeger *et al.*, "Poisson model of spike generation," *Handout, University of Stanford*, vol. 5, no. 1-13, p. 76, 2000.
- [32] N. A. Ibraheem, M. M. Hasan, R. Z. Khan, and P. K. Mishra, "Understanding color models: a review," *ARPN Journal of science and technology*, vol. 2, no. 3, pp. 265–275, 2012.
- [33] K. N. Plataniotis, "Color image processing and applications," *Measurement Science and Technology*, vol. 12, no. 2, pp. 222–222, 2001.
- [34] H.-K. Kim, J. H. Park, and H.-Y. Jung, "An efficient color space for deep-learning based traffic light recognition," *Journal of Advanced Transportation*, vol. 2018, no. 1, p. 2365414, 2018.
- [35] M. Chyad, B. Zaidan, A. Zaidan, H. Pilehkouhi, R. Aalaa, S. Qahtan, H. A. Alsattar, D. Pamucar, and V. Simic, "Exploring adversarial deep learning for fusion in multi-color channel skin detection applications," *Information Fusion*, vol. 114, p. 102632, 2025.
- [36] Y. Liu, J. Dong, and P. Zhou, "Defending against adversarial attacks in deep learning with robust auxiliary classifiers utilizing bit-plane slicing," *ACM Journal on Emerging Technologies in Computing Systems (JETC)*, vol. 18, no. 3, pp. 1–17, 2022.
- [37] G. Chen, Y. Chen, Z. Yuan, X. Lu, X. Zhu, and W. Li, "Breast cancer image classification based on cnn and bit-plane slicing," in *2019 International Conference on Medical Imaging Physics and Engineering (ICMIPE)*. IEEE, 2019, pp. 1–4.
- [38] J. Gautrais and S. Thorpe, "Rate coding versus temporal order coding: a theoretical approach," *Biosystems*, vol. 48, no. 1-3, pp. 57–65, 1998.
- [39] Y. Kim, H. Park, A. Moitra, A. Bhattacharjee, Y. Venkatesha, and P. Panda, "Rate coding or direct coding: Which one is better for accurate, robust, and energy-efficient spiking neural networks?" in *ICASSP 2022-2022 IEEE International Conference on Acoustics, Speech and Signal Processing (ICASSP)*. IEEE, 2022, pp. 71–75.
- [40] B. Han and K. Roy, "Deep spiking neural network: Energy efficiency through time based coding," in *European conference on computer vision*. Springer, 2020, pp. 388–404.
- [41] K. Alex, "Learning multiple layers of features from tiny images," <https://www.cs.toronto.edu/kriz/learning-features-2009-TR.pdf>, 2009.
- [42] A. Paszke, S. Gross, F. Massa, A. Lerer, J. Bradbury, G. Chanan, T. Killeen, Z. Lin, N. Gimelshein, L. Antiga *et al.*, "Pytorch: An imperative style, high-performance deep learning library," *Advances in neural information processing systems*, vol. 32, 2019.
- [43] W. Fang, Y. Chen, J. Ding, Z. Yu, T. Masquelier, D. Chen, L. Huang, H. Zhou, G. Li, and Y. Tian, "Spikingjelly: An open-source machine learning infrastructure platform for spike-based intelligence," *Science Advances*, vol. 9, no. 40, p. eadi1480, 2023. [Online]. Available: <https://www.science.org/doi/abs/10.1126/sciadv.adi1480>
- [44] E. Riba, D. Mishkin, D. Ponsa, E. Rublee, and G. Brádski, "Kornia: an open source differentiable computer vision library for pytorch," in *Winter Conference on Applications of Computer Vision*, 2020. [Online]. Available: <https://arxiv.org/pdf/1910.02190.pdf>
- [45] D. P. Kingma and J. Ba, "Adam: A method for stochastic optimization," *arXiv preprint arXiv:1412.6980*, 2014.
- [46] P. Helber, B. Bischke, A. Dengel, and D. Borth, "Eurosat: A novel dataset and deep learning benchmark for land use and land cover classification," *IEEE Journal of Selected Topics in Applied Earth Observations and Remote Sensing*, vol. 12, no. 7, pp. 2217–2226, 2019.
- [47] F.-F. Li, M. Andreeto, M. Ranzato, and P. Perona, "Caltech 101," Apr 2022.
- [48] G. Griffin, A. Holub, and P. Perona, "Caltech 256," Apr 2022.
- [49] J. Howard, "Imagenette." [Online]. Available: <https://github.com/fastai/imagenette/>
- [50] J. Deng, W. Dong, R. Socher, L.-J. Li, K. Li, and L. Fei-Fei, "Imagenet: A large-scale hierarchical image database," in *2009 IEEE conference on computer vision and pattern recognition*. Ieee, 2009, pp. 248–255.
- [51] J. Stallkamp, M. Schlipsing, J. Salmen, and C. Igel, "Man vs. computer: Benchmarking machine learning algorithms for traffic sign recognition," *Neural Networks*, no. 0, pp. –, 2012. [Online]. Available: <http://www.sciencedirect.com/science/article/pii/S0893608012000457>
- [52] L. Bossard, M. Guillaumin, and L. Van Gool, "Food-101 – mining discriminative components with random forests," in *European Conference on Computer Vision*, 2014.
- [53] L. Deng, "The mnist database of handwritten digit images for machine learning research [best of the web]," *IEEE signal processing magazine*, vol. 29, no. 6, pp. 141–142, 2012.
- [54] H. Xiao, K. Rasul, and R. Vollgraf, "Fashion-mnist: a novel image dataset for benchmarking machine learning algorithms," *arXiv preprint arXiv:1708.07747*, 2017.
- [55] T. Clanuwat, M. Bober-Irizar, A. Kitamoto, A. Lamb, K. Yamamoto, and D. Ha. (2018) Deep learning for classical japanese literature.

APPENDIX

This section contain the training progression graph for each variant of experiments in Section VII-A and Section VII-B. It is noteworthy from Figure 3 and 4 that performance fluctuations were observed in both traditional encoding and our encoding method. We hypothesize that these fluctuations are due to variations in Poisson-distributed spike trains [3]. While our encoding method appears to reduce these fluctuations in certain datasets, such as in Imagenette [49], there are still performance degradation on different variants of the encoder on GTSRB [51].

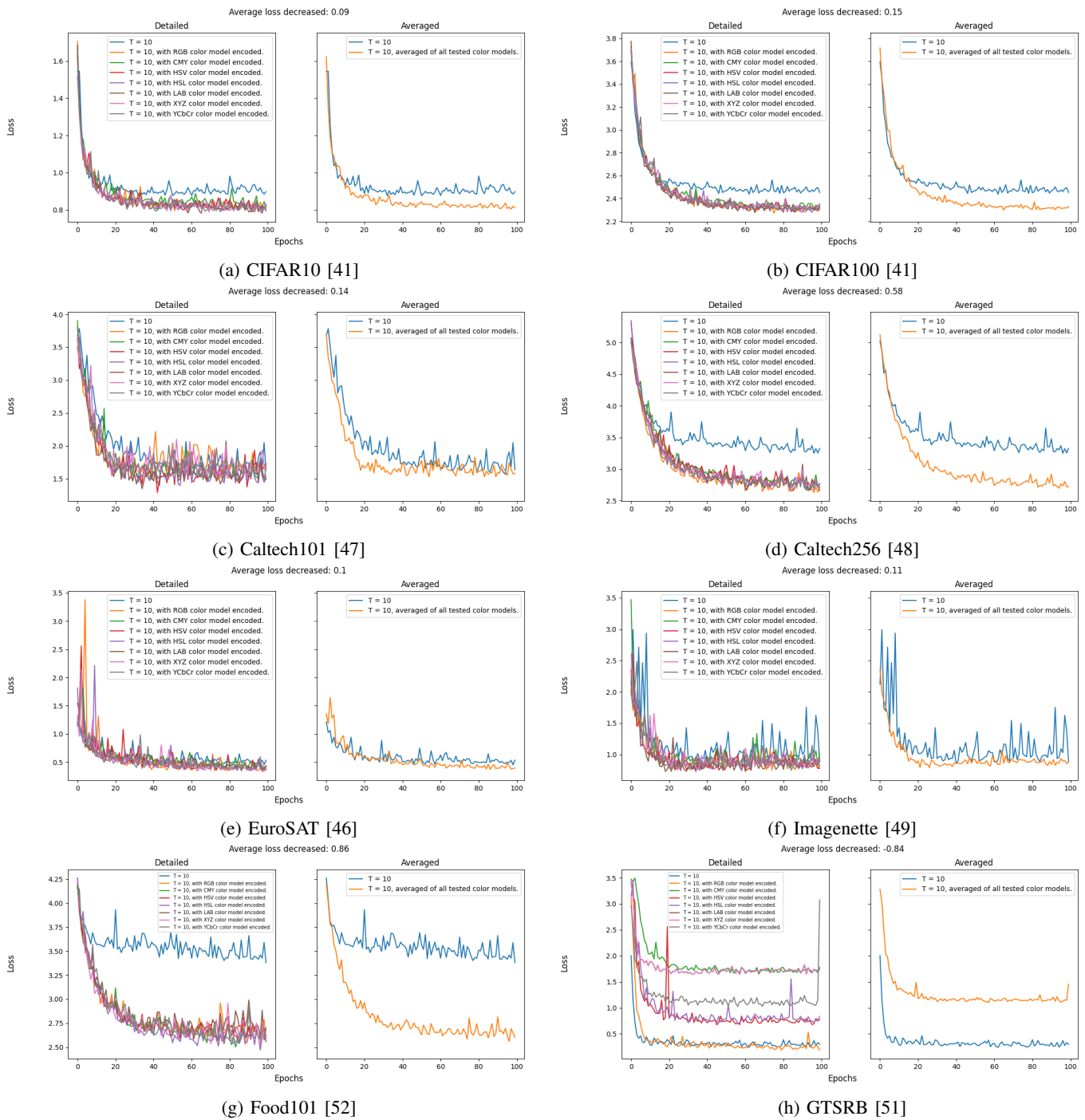
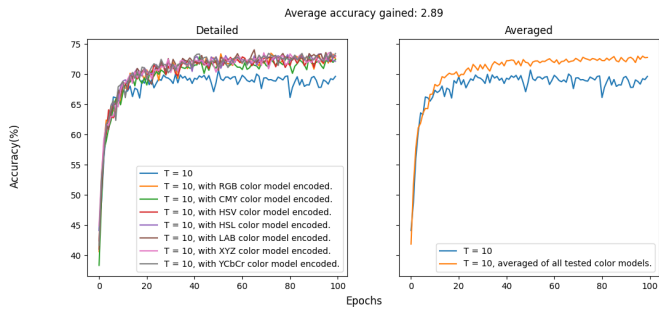
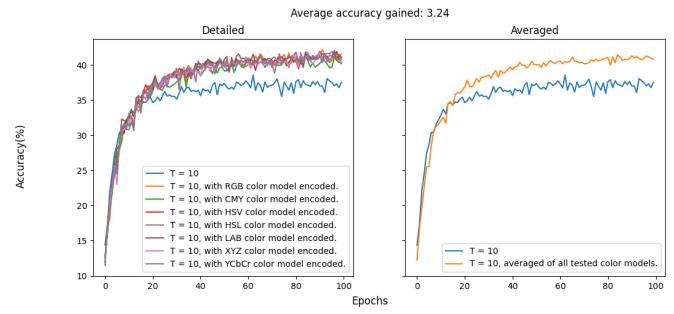


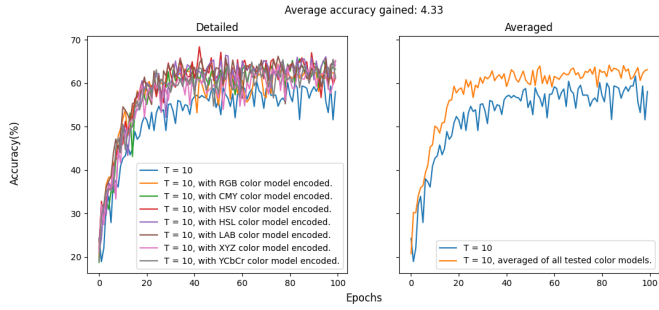
Fig. 3: Comparison in loss progression of traditional rate coding with our method on image classification datasets. On every sub-figure, loss details of every color models is shown on the left and average result of all models on the right with maximum loss difference denoted on top of figure.



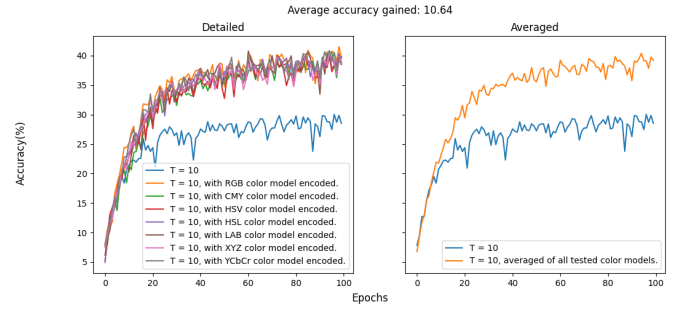
(a) CIFAR10 [41]



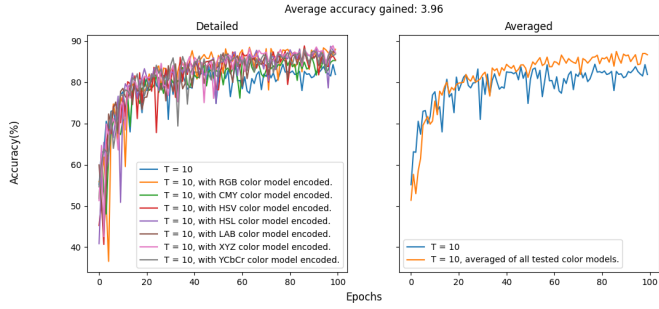
(b) CIFAR100 [41]



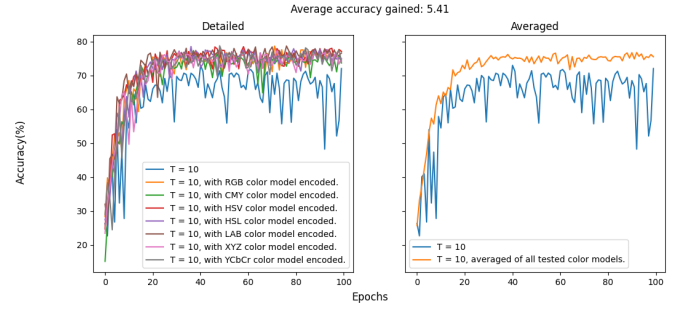
(c) Caltech101 [47]



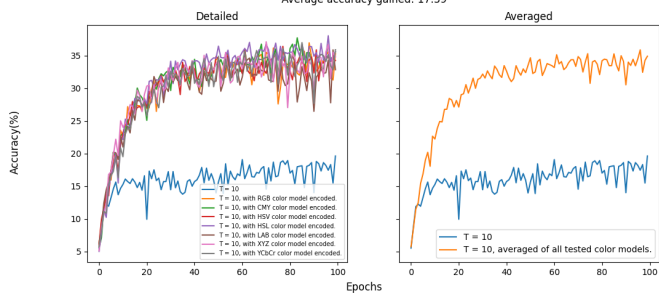
(d) Caltech256 [48]



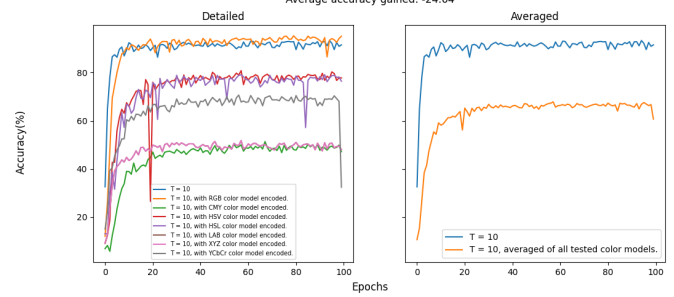
(e) EuroSAT [46]



(f) Imagenette [49]

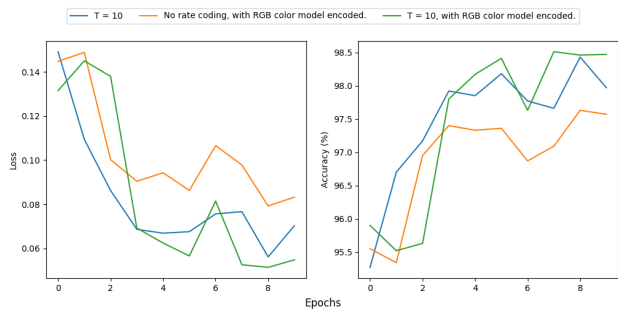


(g) Food101 [52]

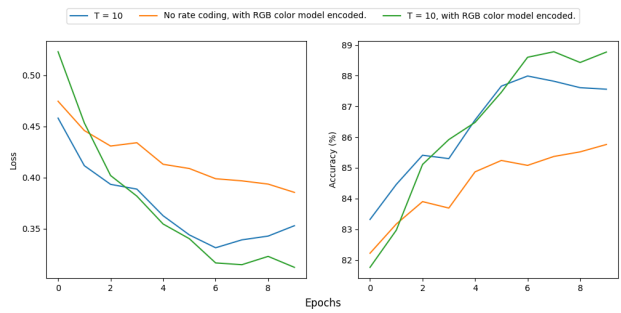


(h) GTSRB [51]

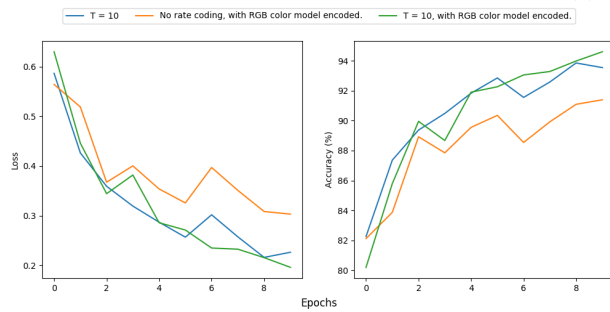
Fig. 4: Comparison in accuracy progression of traditional rate coding with our method on image classification datasets. On every sub-figure, accuracy details of every color models is shown on the left and average result of all models on the right with maximum accuracy difference denoted on top of figure.



(a) MNIST



(b) Fashion-MNIST



(c) KMNIST

Fig. 5: Comparison in accuracy progression and loss progression between encoding methods on different low-resolution gray-scale image classification datasets.